INFLUENCE OF THE YUKON RIVER ON THE BERING SEA
Final Report

Kenneson G. Dean
Geophysical Institute

C. Peter McRoy
Institute of Marine Science

University of Alaska
Fairbanks, Alaska 99775-0800

ABSTRACT

Physical and biological oceanography of the northern Bering Sea including the influence of the Yukon River were studied using satellite data in conjunction with shipboard measurements. The satellite data acquired by the NOAA Advanced Very High Resolution Radiometer (AVHRR), the Landsat Multispectral Scanner (MSS) and the Thematic Mapper (TM) sensor were used to detect sea surface temperatures and suspended sediments. Shipboard measurements of temperature, salinity and nutrients were acquired through the Inner Shelf Transfer and Recycling (ISHTAR) project and were compared to digitally enhanced and historical satellite images.

The satellite data reveal north-flowing, warm water along the Alaskan coast that is highly turbid with complex patterns of surface circulation near the Yukon River delta. To the west near the Soviet Union, cold water, derived from an upwelling, mixes with shelf water and also flows north. The cold and warm water coincide with the Anadyr, Bering Shelf and Alaskan Coastal water masses. The Anadyr water mass is cold (-1 to 6° C), highly saline (31.7 to 33 °/oo) and nutrient rich. In contrast, the Alaskan Coastal water mass is warm (2 to 12° C) has low salinity (less than 31.7 °/oo) and is nutrient poor, but has high concentrations of suspended sediments in the vicinity of the Yukon Delta.

Generally satellite-derived sea surface temperatures were higher than field measurements. Although water masses are primarily defined by salinity , satellite images can be used to define the core of the water mass, where temperature is highly correlated to salinity, rather than water mass boundaries where the correlation can be poor. Patterns of phytoplankton biomass and productivity are determined by mixing of water masse correlate reasonably well with the pattern if surface isotherm distribution obtained from satellite images.

Historical satellite images (1974 to 1978) were used to investigate the variability of the warm and cold surface water. Generally, warm Alaskan Coastal Water forms near the coast and extends offshore as the summer progresses. Turbid water discharged by the Yukon River progresses in the same fashion but extends northward across the entrance to Norton Sound, attaining its maximum surface extent in October. The Anadyr Water flows northward and around St. Lawrence Island; but its extent is highly variable and depends upon mesoscale pressure fields in the Arctic Ocean and the Bering Sea.

INTRODUCTION

The continental shelf of the Bering and Chukchi seas adjacent to northwest Alaska and northeastern Siberia (Fig. 1) consists of a broad plateau typically less than 50 m deep. The marine environment is characterized by a strongly advective physical regime that consists of three water masses flowing around St. Lawrence Island north through Bering Strait: Anadyr,
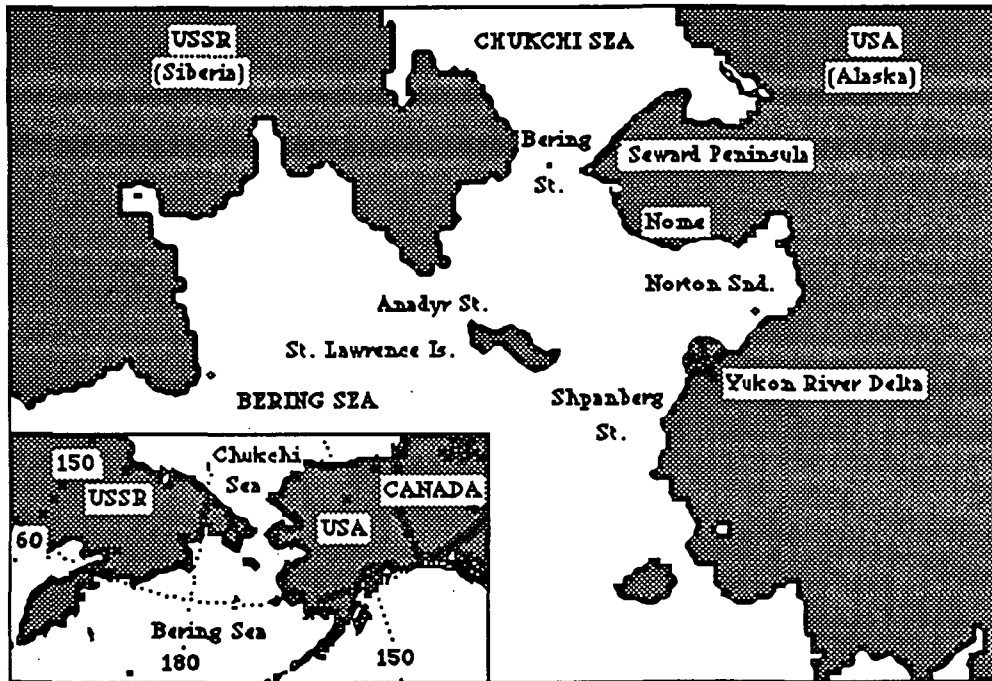
1

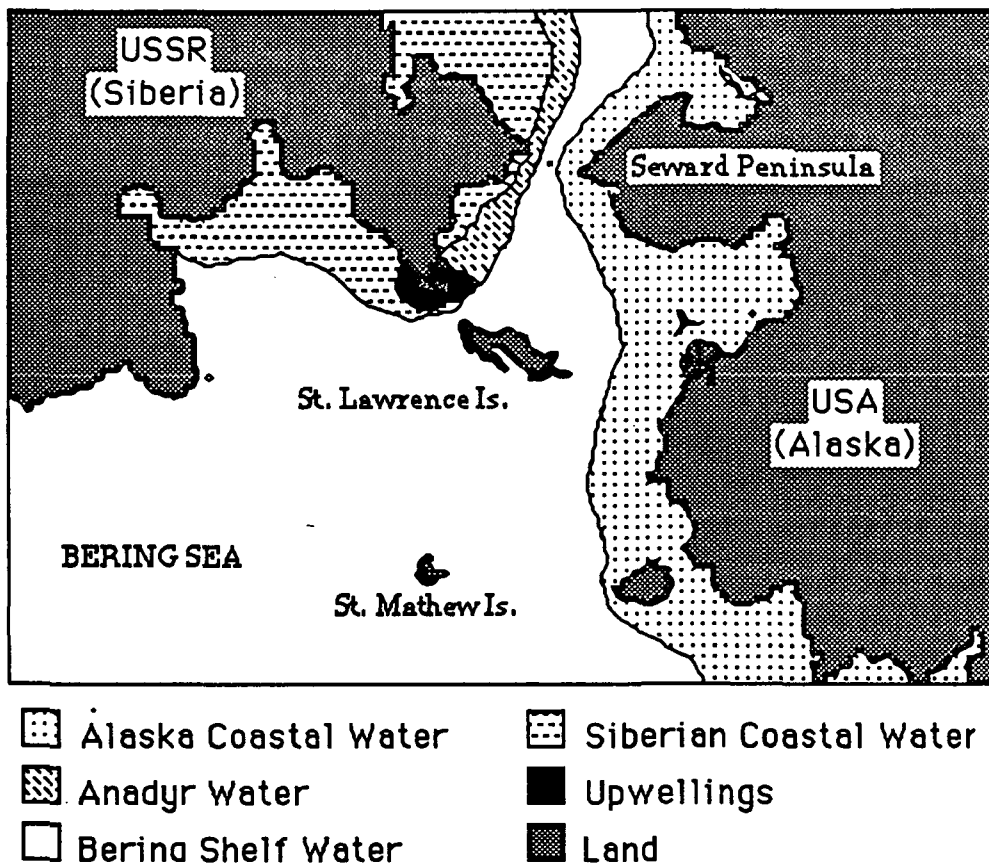*Figure 1. Location diagram of the Bering Sea.*

Figure 2. Generalized distribution of water masses in the Bering and Chukchi seas. Upwellings typically develop in the locations shown as seen on thermal infrared AVHRR satellite imagery.

Bering Shelf and Alaskan Coastal (Fig. 2). These water masses constitute the flow from the Bering Sea to the Chukchi Sea (Coachman et al., 1975). This flow is almost always northward and is driven by the fundamental pressure difference between the North Pacific and North Atlantic oceans. Occasionally flow reversals occur under certain meteorological conditions.

Anadyr Water, which originates at depth along the continental slope, advects abundant nutrients (especially nitrate) and biota into the western portion of the region and is responsible for highly productive benthic and pelagic food webs. Bering Shelf Water, which flows between the Anadyr and Alaskan Coastal water masses, originates on the northern shelf of the Bering Sea and thus has a low nutrient content. Alaskan Coastal Water is a low salinity, seasonally warm coastal current originating on the inner shelf of the southeastern Bering Sea. Since this too has low nutrients, it is less productive than waters influenced by the Anadyr stream. Alaskan Coastal Water is modified by the discharge of the Yukon River, which further dilutes the flow, particularly in early summer following ice breakup. At the same time it also adds measurable heat to an environment still cold from winter. The ascension of energy from the primary producers to upper trophic levels in the coastal zone of northwest Alaska apparently is correlated to patterns of seasonal warming.

Satellite imagery provides a synoptic view of the Bering Sea that records sea surface temperatures (SST) and radiances from which surface circulation and distribution can be inferred. The sensors "freeze" the motion of dynamic hydrologic environments and thus provide a data source to study relationships among various features. The diversity of orbiting satellites result in the recording of image swaths ranging in widths from about 2200 km (Advanced Very High Resolution Radiometer-AVHRR) providing a very broad perspective at 1 km resolution to 185 km (Landsat) providing a more localized perspective at 30 to 120 m resolution. The satellites also differ in the frequency of repetitive coverage from daily (AVHRR) to every 16 days excluding side lap (Landsat 4 and 5). The repetitious coverage provides valuable data for monitoring some oceanic processes (Thomas, 1980). These satellites have detectors sensitive to visible, infrared and thermal infrared radiation that have recorded a variety of oceanographic conditions in the Bering and Chukchi region including sea-surface temperature (Springer et. al., 1987; Springer et. al., 1984; Ahlnas and Garrison., 1984; and Coachman et. al. 1975), turbidity (Sharma, 1979 and Burbank, 1974) and sea ice conditions (Stringer and Groves, 1985). The purpose of this project was to incorporate the synoptic view provided by satellite data with ship-board measurements into a study of the ecosystem of the northern Bering Sea shelf, most specifically the influence of the Yukon River on this environment, and to evaluate the utility of the new Landsat Thematic Mapper data for oceanographic and marine ecosystem studies.

METHODS

NOAA AVHRR, Landsat Multispectral (MSS) and Landsat Thematic Mapper (TM) data were acquired of the northern Bering Sea during ice free periods of 1985 through 1987. Throughout this same period, samples and measurements were collected within the water column from oceanographic research vessels by investigators from the Inner Shelf Transfer and Recycling project (ISHTAR). ISHTAR is a National Science Foundation (NSF) funded project studying biological productivity and ecosystem processes of this northern shelf area. The shipboard measurements were used to calibrate the satellite data and to provide direct field measurements of temperature, salinity, nutrients and productivity within the water column.

The satellite data were digitally enhanced to optimize the analysis of sea surface temperature, currents, circulation and suspended sediment load. Processing consisted of masking the land areas and clouds, filtering to minimize noise, and enhancing image contrast (contrast stretch) to display subtle patterns and structures in the image. Spectral bands were enhanced individually, and composited for interpretation. Principal components analysis and band ratios were applied to TM data to enhance turbid water. To quantify the extent of intensity differences on the sea surface, discrete levels of image brightness were color coded, referred to as level slicing, such that continuous geometric patterns were formed on the images. The radiometric range of the level slices were kept constant for each data type

except at the extremities where additional levels were added when needed as the dynamic range of the water fluctuated due to environmental conditions. The color ranges on the level slice show extent and relative differences in either water temperature, in the case of thermal spectral bands, or suspended sediment concentrations in visible spectral bands. The AVHRR data were registered to a bathymetric base-map and transformed to an Alberts Equal Area map projection. The satellite images were not corrected for atmospheric conditions since relative differences were emphasized and field observations and measurements were available from ISHTAR investigators.

The variability of sea surface temperatures and turbid water were also investigated using archived satellite imagery from the 5-year period 1974 through 1978. Surface, temperature-sensitive boundaries of warm and cold water observed on thermal-infrared AVHRR imagery, and the boundaries of turbid water observed on visible bands of AVHRR and MSS imagery were mapped. Over 100 images from each data source were analyzed. Inter-annual and intra-annual variability were summarized by overlaying the resulting maps and generalizing the location of boundaries. These generalizations minimize errors caused by misregistration and the possible lack of continuity in the interpretation of grey tones between images.

RESULTS

AVHRR Data

The thermal infrared channel of the AVHRR sensor provided a synoptic perspective of sea surface temperature in the Bering/Chukchi Seas, revealing a large thermal range of 3 to 19 ^{0} C during mid and late summer (Fig. 3). These temperatures were derived from radiance to temperature look-up tables provided by NOAA. Field measurements of temperature and satellite values were within 1^0 C in some cases, and in others varied by a factor of two. These variations can be attributed to several factors including:

    1. Oceanographic conditions - Some stratification develops in the water column resulting in disparities between surface and subsurface values. Satellite values are derived from the first few micrometers of the water surface and ship-board measurements were acquired at 1 meter or greater;

    2. Differences in the time required to collect data - Satellites acquire a "snap shot" while field measurements were acquired over approximately 20 days.

    3. Meteorological conditions - Wind can expand or contract the extent of water bodies at the surface beyond their normal subsurface distribution.

    4. Atmospheric conditions - Absorption, scatter and emission by gases and particles in the atmosphere can increase or decrease the apparent temperature of the water surface.

Of the factors listed stratified water was the greatest potential problem in that it could mask subsurface conditions, but as shown in figure 3 and verified with field data, it did not cause problems in differentiating the core of the upwelled, shelf and coastal water. However, surface values along the fronts of the waterbodies were not always in agreement with subsurface measurements primarily due to stratification and presumably transport of surface water by wind.

Generally, satellite and field data were in best agreement in the vicinity of the upwelling in Anadyr Strait where differences within the water column were not as extreme as in coastal water. The greatest discrepancy occurred in Alaskan Coastal Water, where water at the surface can become highly stratified because of fresh water discharged by rivers.

The level-sliced images (Fig. 3) reveal cold surface water close to the coast of the Soviet Union especially in Anadyr Strait and a progressively warmer trend eastward to the coast of Alaska. The coldest water (3 to 4^{0}C, dark blue on the images), originates from an upwelling that occurs in Anadyr Strait (near the Soviet coast), and flows northward through Bering Strait on the western side on this shelf. The warmest water (12 to 19^{0}C, yellow-brown-red tones), is adjacent to the Alaskan coast especially in Norton Sound, also flows northward and remains in the eastern Bering Sea. Temperatures as high as 22.5 ^{0}C, grey tones, were recorded on the
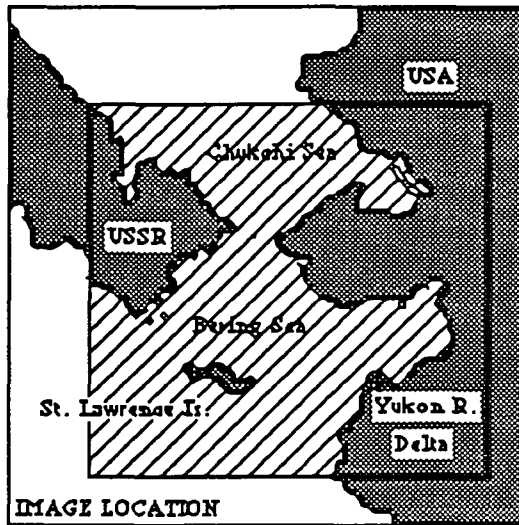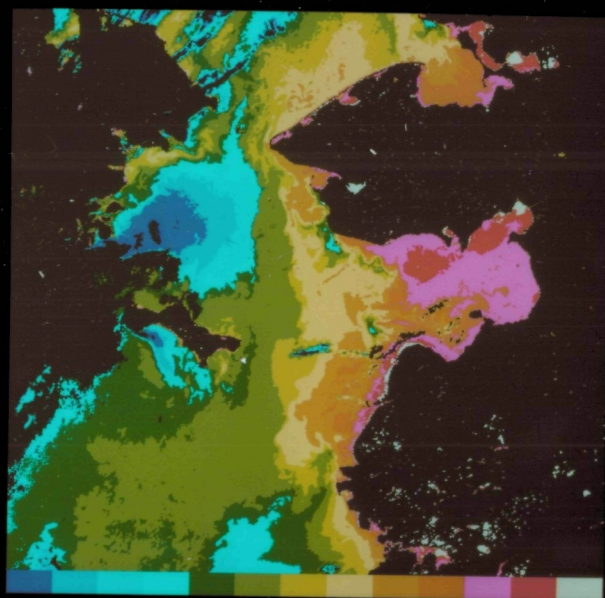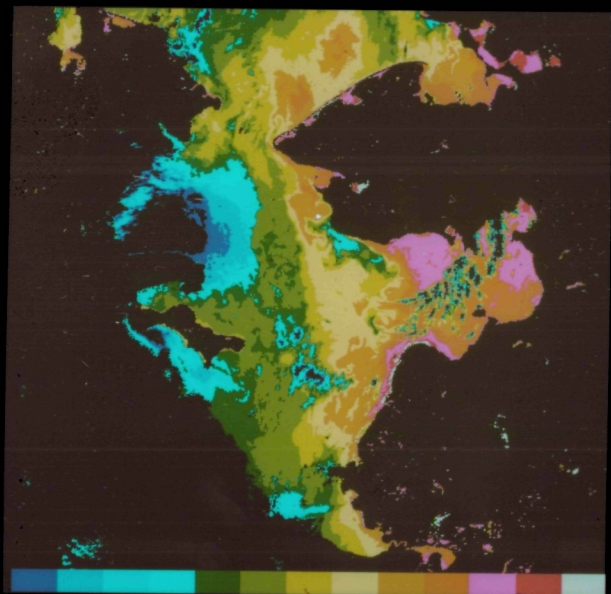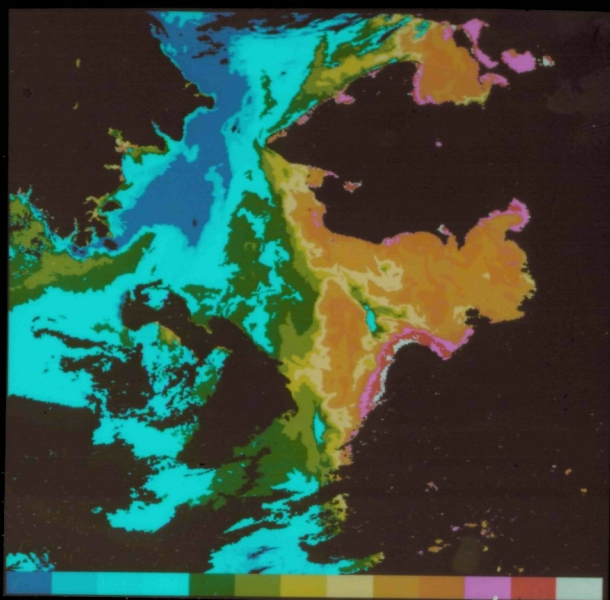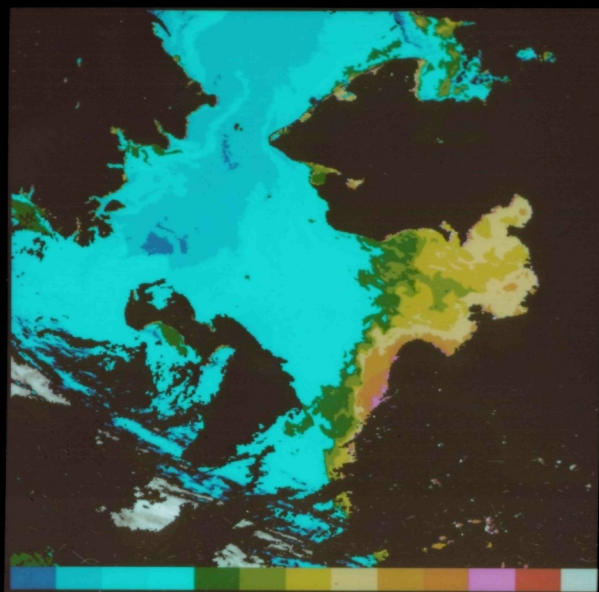
Figure 3. Time series AVHRR satellite images of the Bering and Chukchi seas, summer 1985: upperleft -5 July (Orbit 11802 N8); upper right-22July (Orbit 03126 N9); lower left-2 August (Orbit 03281); lower right 3 August (Orbit 03295). These thermal infrared images have been level sliced to emphasize relationships between surface temperature and underlying water masses.

images in a few, very limited areas immediately adjacent to the Alaskan coast . Some warm water also develops adjacent to the Soviet coast south of Bering Strait and occasionally extends northward into the Chukchi Sea. Modified Bering Shelf water in the central shelf, light blue and green tones, has intermediate temperatures (6 to 11°C) and also flows north.

The sequence of images from 1985 (Fig. 3) shows daily and monthly variations in the distribution and geometry of the coastal and upwelled water as seen at the surface. The warm coastal water extends westward as the summer progresses and stabilizes in the vicinity of the 30 m isobath. The images also show that the cold upwelled water originates in Anadyr Strait near the coast of the USSR with the temperature range remaining constant. The extent and shape of this water mass is variable but for the most part it remains in the western Bering and Chukchi seas. Field data indicate that the position of the eastward front of the upwelled water is variable throughout the water column.

Landsat MSS Data

Landsat MSS data provide a more restrictive, but still regional, perspective of the oceanic environment compared to the AVHRR data. The visible red channel (band 2) of the MSS data was used to examine the distribution of turbid water near the surface that is discharged by the Yukon River. Penetration of turbid water by red-visible wavelengths ranges from 45 cm (Thomas, 1980) to 1-2 m (Burbank, 1974). Water depths in the study area exceed these depths except in the immediate vicinity of the coast and possibly over shoals and sand bars.

A level sliced image (Fig. 4) of the Yukon River outflow recorded on 5 July 85 reveals the distribution and circulation of turbid water. The colors represent increasing degrees of brightness of the water caused by turbidity from blue through cyan, magenta, red, green and yellow. The turbidity is primarily caused by suspended sediments, mostly silt with fine sand and clay (Burbank, 1974). Suspended-sediment concentrations of 700 mg/l have been measured in the Yukon River near the delta at Pilot Station (U.S. Geol. Surv. Water Data, 1975 to 1978) and near-surface concentrations as great as 30 mg/l have been measured several kilometers offshore from the delta (Drake et. al., 1980). The distribution of modern bottom sediments (Nelson, 1982) approximately coincides with the extent of the turbid water displayed on the images, suggesting that the circulation shown by the image is representative of the area and that there are no significant changes in circulation patterns at depth.

The imagery reveals that most of the turbid water is flowing north and northwest across the entrance to Norton Sound with lesser amounts circulating into the sound. To the west, the highest brightness levels (yellow) occur offshore near the edge of the delta-front platform described by Dupre (1982) rather than in the immediate vicinity of the delta. Breakers form when waves encounter shoals and the relatively shallow delta-front platform. Apparently, resuspension of sediments and mixing of turbid, subsurface water by wave action result in more highly turbid water at the surface offshore than where expected nearshore in the vicinity of river channels.

Landsat TM Data

The TM data has higher resolution (30 m in reflective bands and 120 m in the thermal-infrared band) than the AVHRR and MSS data, and thus provide valuable information concerning local circulation and mixing but have a limited field of view compared to the AVHRR data. This can be seen by comparing the level-sliced, thermal infrared AVHRR image (Fig. 3) and TM image (Fig. 5) recorded within approximately fourteen hours of each other on 5 July 85. Numerous scalloped and tongue-shaped structures at the surface can be seen on the TM thermal image that are related to the mixing of cold oceanic water and warm coastal water. On the AVHRR image only a few of the larger structures can be observed. Differences in the information content of these two data sets are even more apparent in the visible bands
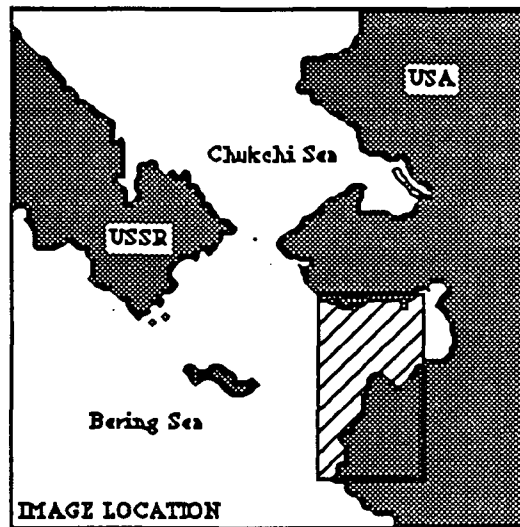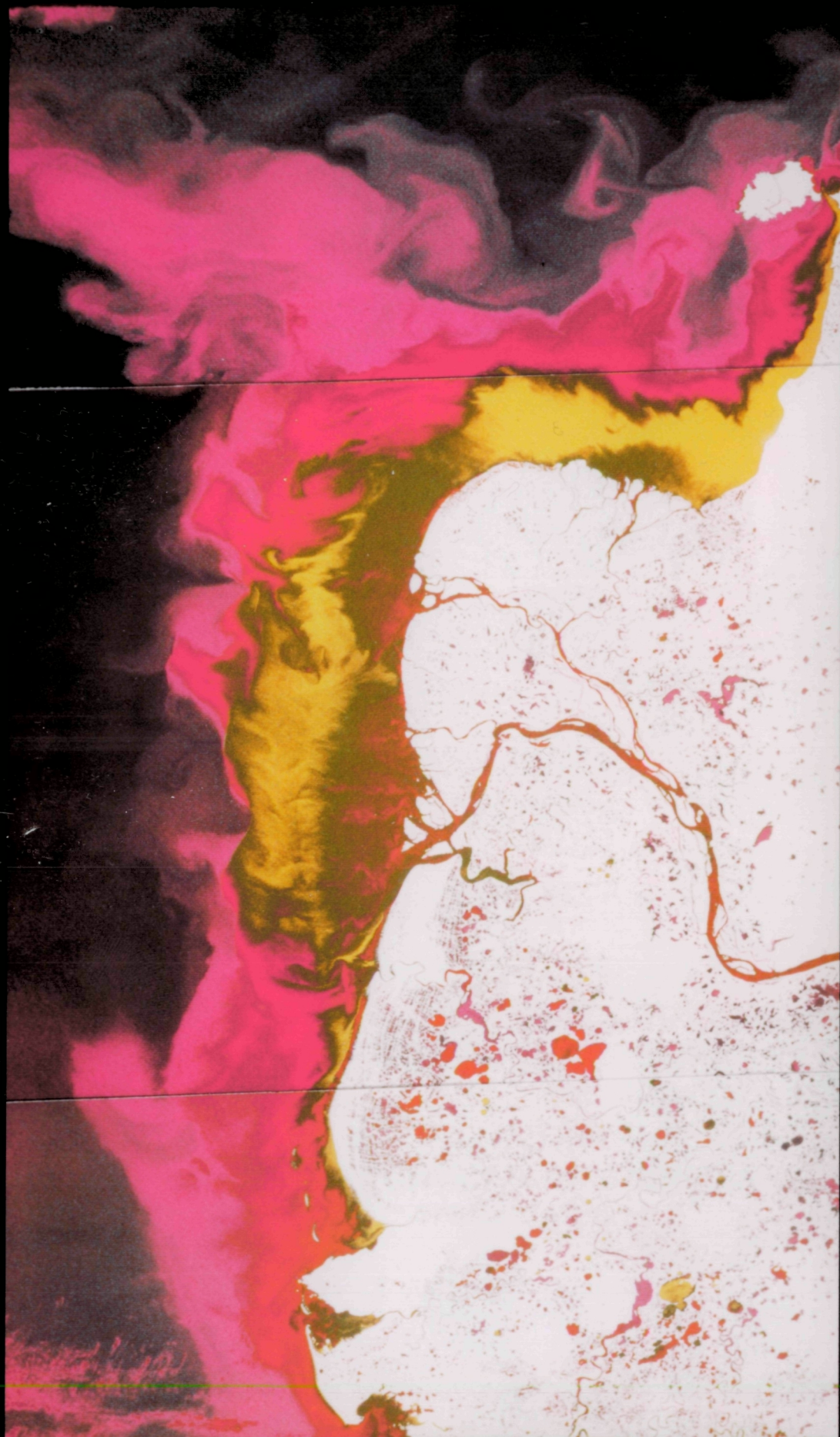
Figure 4. Mosaic of Landsat MSS images of the Yukon River delta and vicinity. The visible-green band images have been level sliced to emphasize turbid water discharged by the Yukon River into the Bering Sea and Norton Sound. Scene ID's: 41085-21395, 41085-21393, 41085-2139; 5 July 85 (processed by UAF Landsat Quick-Look Program).

where the TM resolution is greater yet.

The TM image (Fig. 5) covers the boundary between cold shelf and cool coastal waters (blue and green tones), and warm coastal water (red and yellow tones). At the surface river water discharged by the Yukon River circulates into Norton Sound (to the right) along the southern coast and out along the northern coast in a cyclonic pattern. A tongue of cooler water from the shelf extends into the center of the Sound. The surface circulation is based on the direction that eddies curl along the front between the intruding shelf and coastal water, and eddies that form where land disrupts the flow. The temperature of the warm water discharged by the Yukon River decreases as the distance offshore from the delta increases. This temperature change with distance is in good agreement with trajectory and dilution numerical models of buoyant surface jets (Gosink,1988).

The thermal-band TM image (Fig. 5) and the visible-band MSS image (Fig.4) recorded within approximately fourteen hours of each other on 5 July 85 reveal somewhat different circulation patterns of Yukon River water. The visible-band data (see Landsat MSS Data) shows that most of the turbid Yukon water flows across the entrance to Norton Sound. The thermal-band data shows warm Yukon water primarily circulating into and out of Norton Sound. Wind speed and direction, measured at Nome Alaska, were similar at the time of both satellite passes. The TM data were recorded at low tide and MSS at high tide with a tidal range of 1.5 m. Assuming that the winds and tides have not altered the circulation between satellite passes, the differences can be attributed to the depth of penetration of the respective wavelengths and stratification of water near the surface. Thus the thermal data shows the circulation of water at the surface based on sea surface temperatures and the visible data shows the circulation of water within a few meters of the surface based on the distribution of suspended sediments.

The level-sliced image (Fig. 5) displays the complexity and temperatures of structures on the water surface with values ranging from 6.5 degrees C (dark blue) northwest of the Yukon Delta to 13.5 degrees C (dark brown) adjacent to the delta. The temperatures have not been corrected for atmospheric conditions but are in good agreement with field observations. The conversion from radiometric to thermal values are derived from

$$L_b = \frac{(RMAX-RMIN)}{255} D_{cor,b} + RMIN$$

where L_b is temperature in Kelvin, $D_{cor,b}$ is a corrected digital number for band 6, and RMAX and RMIN are derived from radiometric look-up tables (NASA, 1984). The look-up tables in the NASA reference are incorrectly labeled or the sensors had not been recalibrated at that time and hence the captions need to be reversed. This observation is based on a comparison of field measurements with the calculated values.

In contrast to the thermal image which records temperatures at the water surface, the visible band images record turbidity in the first few meters of the water column. Data from band 3 was preferred over bands 1, 2 and 4 for analysis of turbidity structures and circulation, although there were only slight differences in the first three bands. Extreme contrast enhancements of the mid-infrared bands (5 and 7) unexpectedly revealed some structures in the water. Some of the structures seen on the band 5 enhancement correspond to turbidity features on bands 1, 2 and 3, but others were unique. Structures seen on the band 7 image were very subtle and relate more to features on the thermal band than any of the others.

Principal components analysis and band ratios of TM data recorded on 22 July 85 were used to enhance turbid water a few kilometers northeast of the delta. Band ratio 1/3 was preferred to 1/2. A color composite of the first three principal components (Fig. 6A) and a composite of the first two principal components and band ratio, 1/3, (Fig. 6B) significantly enhanced intricate structures within the turbid water. These structures indicate near-surface circulation patterns and differences in suspended sediment concentrations, and possibly the influence of bathymetry on circulation of turbid water.
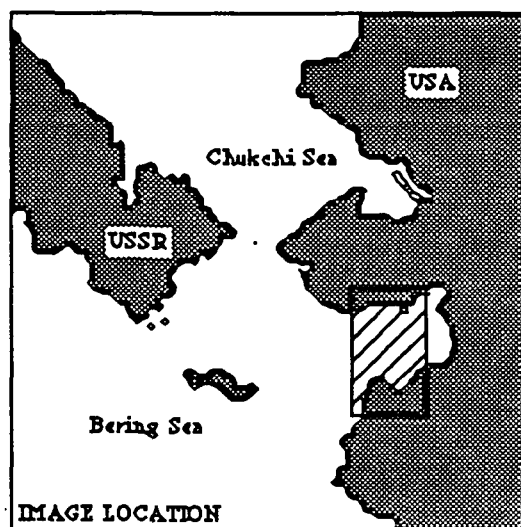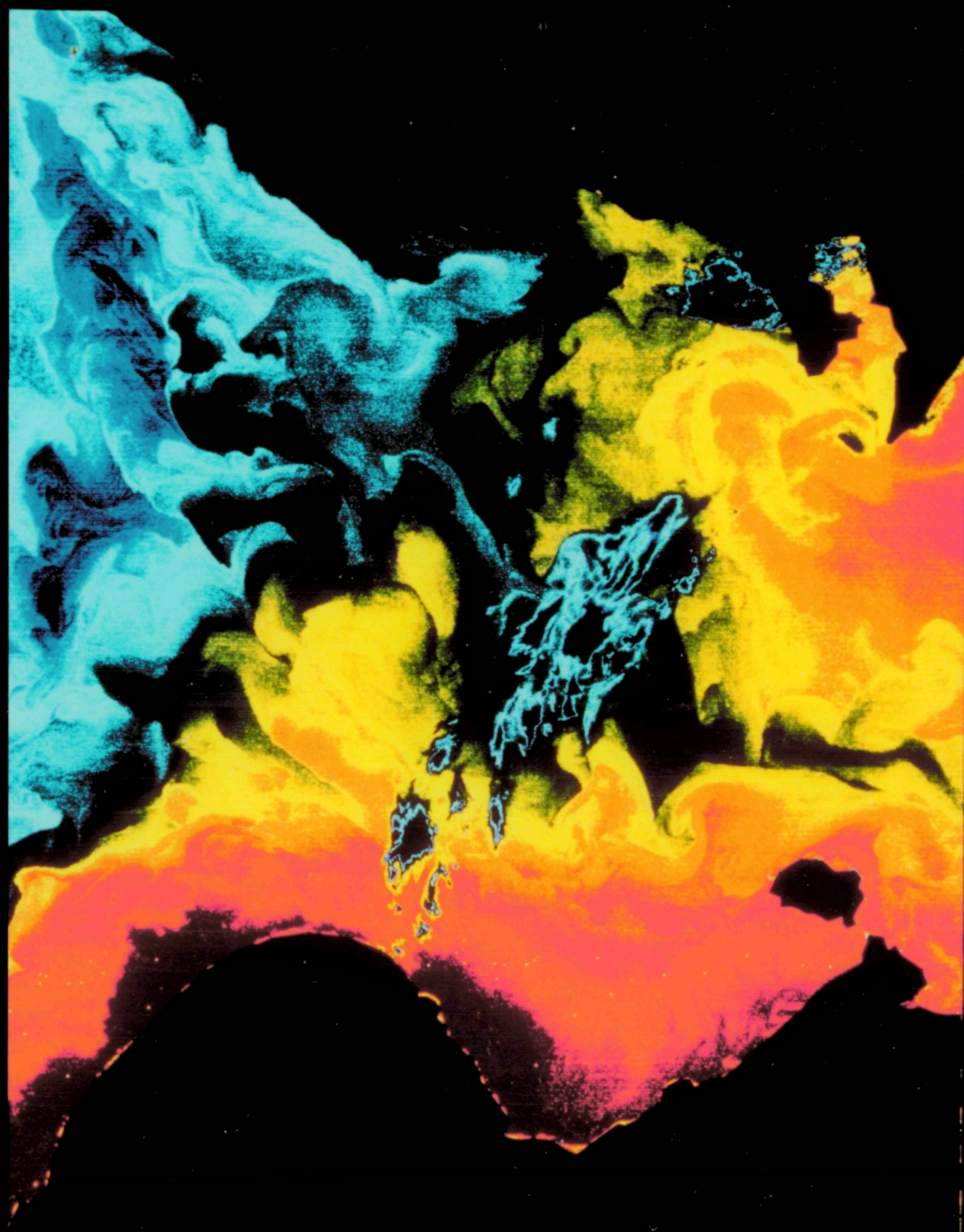
Figure 5. Mosaic of Landsat TM images of the Yukon River delta and vicinity. The thermal images have been level sliced to emphasize structures in the water derived from mixing and dilution of fresh warm water discharged by the Yukon River with shelf water. Scene ID's: 50491-07302 and 50491-07304; 5 July 85 (processed by NASA-GSFC).

LOW
83
84
85
86
87
88
89
90
91
92
93
94
95
96
97
98
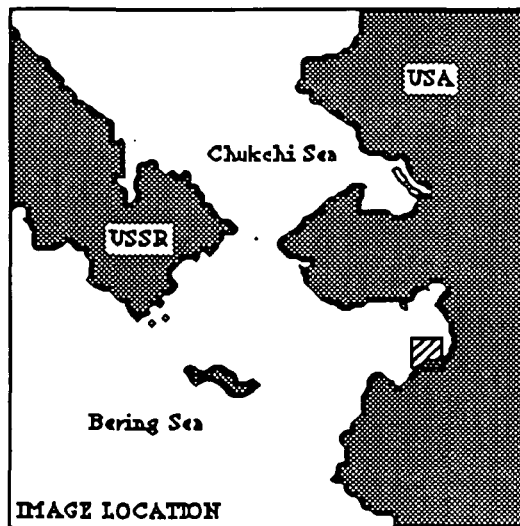99
100
101
102
103
104
105
106
107
108
109
110
111
112
HI

Figure 6. Subsections of Landsat TM data northeast of theYukon delta of Stuart Island in Norton Sound. The visible band images show the distribution and circulation of turbid water. The upper left image is a color composite of the first three principal components. The lower image is a color composite of the first two principal components and band ratio 1/3. Scene ID: 50508-21383; 22 July 85.

Inter-annual Variations

The extent and boundaries of the temperature-sensitive water bodies as observed on historical AVHRR imagery (1974 to 1978) vary substantially as the summer progresses (Fig. 7). These intra-annual changes were similar from year to year. Generally, in early June Alaskan Coastal Water develops near shore in the immediate vicinity of the Yukon delta, to the south along the coast, and in discreet areas along the shore of Norton Sound. By late June the Yukon water has extended northward along the coast into Norton Sound incorporating other warm bodies of water along shore, forming a single water-body. By late July the warm water extends throughout most of Norton Sound and to the north along Alaska's coast approaching the Bering Strait. In August and September the warm water advances seaward, where it stabilizes in the vicinity of the 30 m isobath approximately 100 km offshore from the Yukon delta. Ahlnäs and Garrison (1984) discuss the origin of this warm coastal water, its variations and its dispersion through the Bering Strait. Their field measurements as well as those by ISHTAR investigators indicate that the warm surface waters extend to a depth of 10-30 m.

The distribution of cold upwelled water adjacent to the Soviet coast (Fig. 7), also fluctuates, although the variations are not as consistent as that of the Alaskan Coastal Water. Generally, upwelling was first observed adjacent to the southern coast of the Soviet Union on early June images. The upwelling probably occurs throughout the ice-free period, but becomes distinct when the surrounding surface water at the surface is warmer than the upwelling. By late June and July the cold water has flowed northward adjacent to the coast and seaward as far as longitude 169°W. The cold surface water often extends northward through the Bering Strait and into the Chukchi Sea July through October. The extent and shape of the surface expression of this upwelled water is highly variable.

The distribution and circulation of turbid water along the Alaskan coast is also variable as indicated by historical MSS imagery, and is related to river discharge of Alaskan streams (Fig. 8). Discharge from the Yukon River is the primary component that contributes to the development of this coastal water in the northern Bering Sea as it flows along the Alaskan coast. The plume of suspended sediments develops in May in the vicinity of the delta. In June and early July, when peak river discharge occurs, turbid water extends 20-50 km offshore and across the entrance to Norton Sound. During July the river discharge begins to decrease. However, the extent of near-surface turbid water continues to expand to approximately 100 km offshore in August and 150 km in October. As winter develops, the extent of the turbid water recedes.
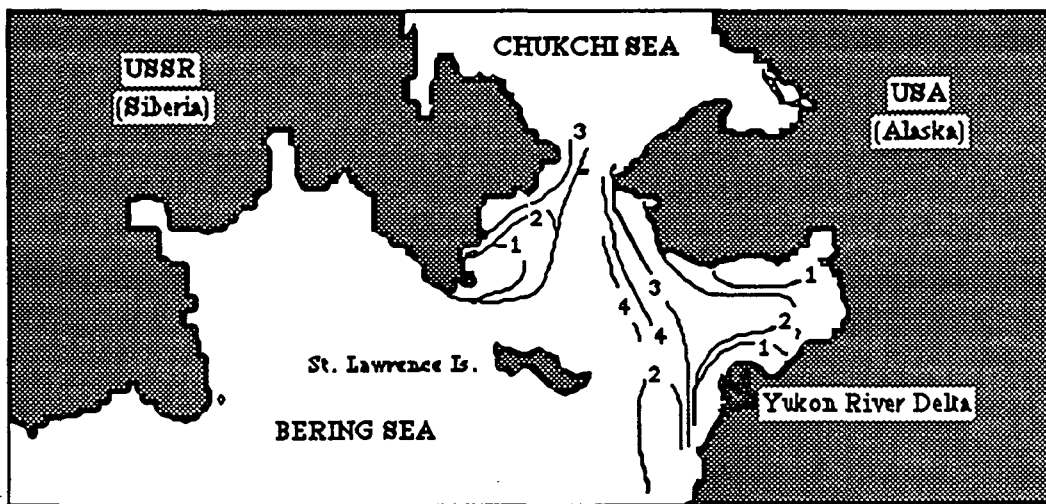
Figure 7. Intra-annual variations in the extent of Alaskan Coastal Water and upwelled water (Anadyr) along the Soviet coast as observed on thermal infrared AVHRR satellite imagery 1974 to 1978. The numbers indicate typical flow sequences of surface fronts that develop during the ice-free period.
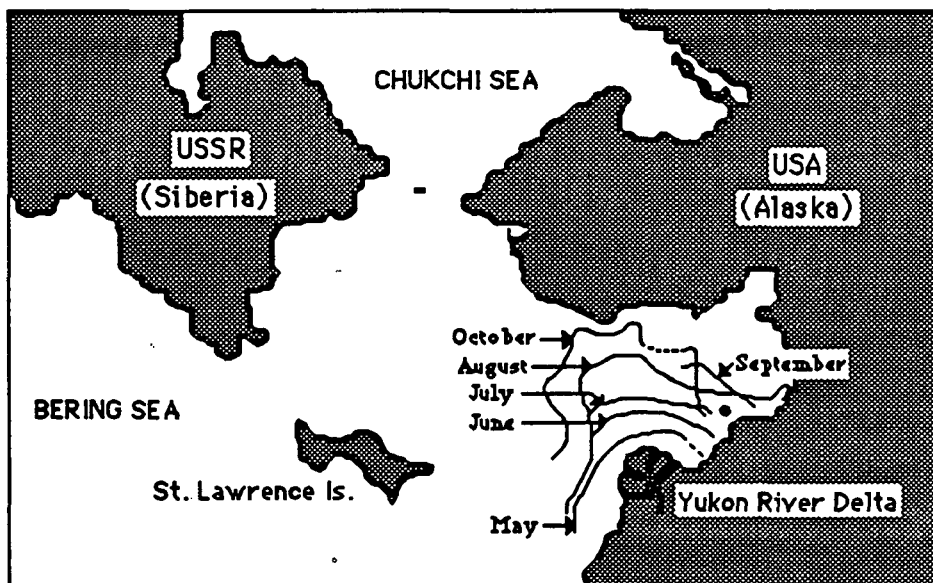

Figure 8. Seasonal variations in the distribution of turbid water discharged by the Yukon River. The integrated analysis is based on historical Landsat MSS imagery (1974 to 1978).

DISCUSSION

The satellite images reveal patterns in the water of the northern shelf of the Bering Sea caused by variations in sea surface temperatures and turbidity. These patterns are primarily related to the circulation and mixing of coastal water, upwelled water and shelf water. Data collected from oceanographic research ships have revealed the presence of three distinct, north-flowing water masses in the northern Bering Sea based on differences in temperature, salinity and nutrients (Coachman et. al., 1975). These water masses are referred to as Alaskan Coastal, Anadyr and Bering Shelf. The Alaskan Coastal Water, is warm (2 to 12 degrees C), has low salinity (less than 31.7 $^o/_{oo}$), is nutrient poor (less than 1 mM nitrate) and has high concentrations of suspended sediments, especially in the vicinity of the Yukon delta. This water is derived from the mixing of Bering Shelf Water with the discharge from streams in western Alaska and is linked to the coastal water in southern Alaska. In contrast, the Anadyr Water is cold (-1 to 6 degrees C), saline (32.5 to 33 $^o/_{oo}$) and nutrient rich (as much as 20 mM of nitrate). The Anadyr Water is derived from an upwelling water that originates in the deep Bering Sea basin. The Bering Shelf Water is formed by winter conditions on the central shelf, and thus has salinity and temperature values between that of the coastal and Anadyr water but low nutrients. The highest primary productivity develops where Bering Shelf Water mixes with Anadyr Water resulting in integrated chlorophyll values in excess of 600 mg/m^2. Patterns of phytoplankton biomass correlate well with the surface temperature distributions from satellite images.

For the most part, the Alaskan Coastal Water near Alaska and Anadyr Water near the Soviet coast observed on the satellite images coincide with the Alaskan Coastal and Anadyr water masses as determined by ship board measurements (Fig. 9 and 10). On figures 10 and 11 the water bodies at the surface were delineated based on sea surface temperatures observed on a AVHRR satellite image (Orbit 13226, 8 July 87). Temperature and salinity values shown in profile were measured on 8 and 9 July 87 (Tripp, 1987). Satellite surface temperatures are in agreement with subsurface measurements to a depth of approximately 10 m. At greater depths the isotherms extend eastward toward Alaska. Generally, the salinity values conform to the position of satellite-derived water bodies in that low values are associated with coastal water and high values with Anadyr water. However, the water mass boundaries are determined by log T/S values which use data from the entire water column. Satellite images identify the core of the water mass rather than the boundaries.

CONCLUSIONS

1. Satellite images provide good synoptic coverage of surface isotherm distribution and show the complicated circulation pattern in the shelf waters of the northern Bering Sea. Since water masses are primarily defined by salinity , satellite images are best used to define the core of the water mass, where temperature is highly correlated to salinity, rather than water mass boundaries where the correlation can be poor.

2. Both AVHRR, MSS and TM reflective band images provide valuable detail in determining the distribution of suspended sediment load and hence circulation patterns related to sediment sources. The plume of the Yukon River can be readily traced by such images and these further reveal complex patterns of surface circulation. The high spatial and spectral resolution of TM provided additional, detailed information regarding marine and coastal processes in the vicinity of the Yukon Delta.
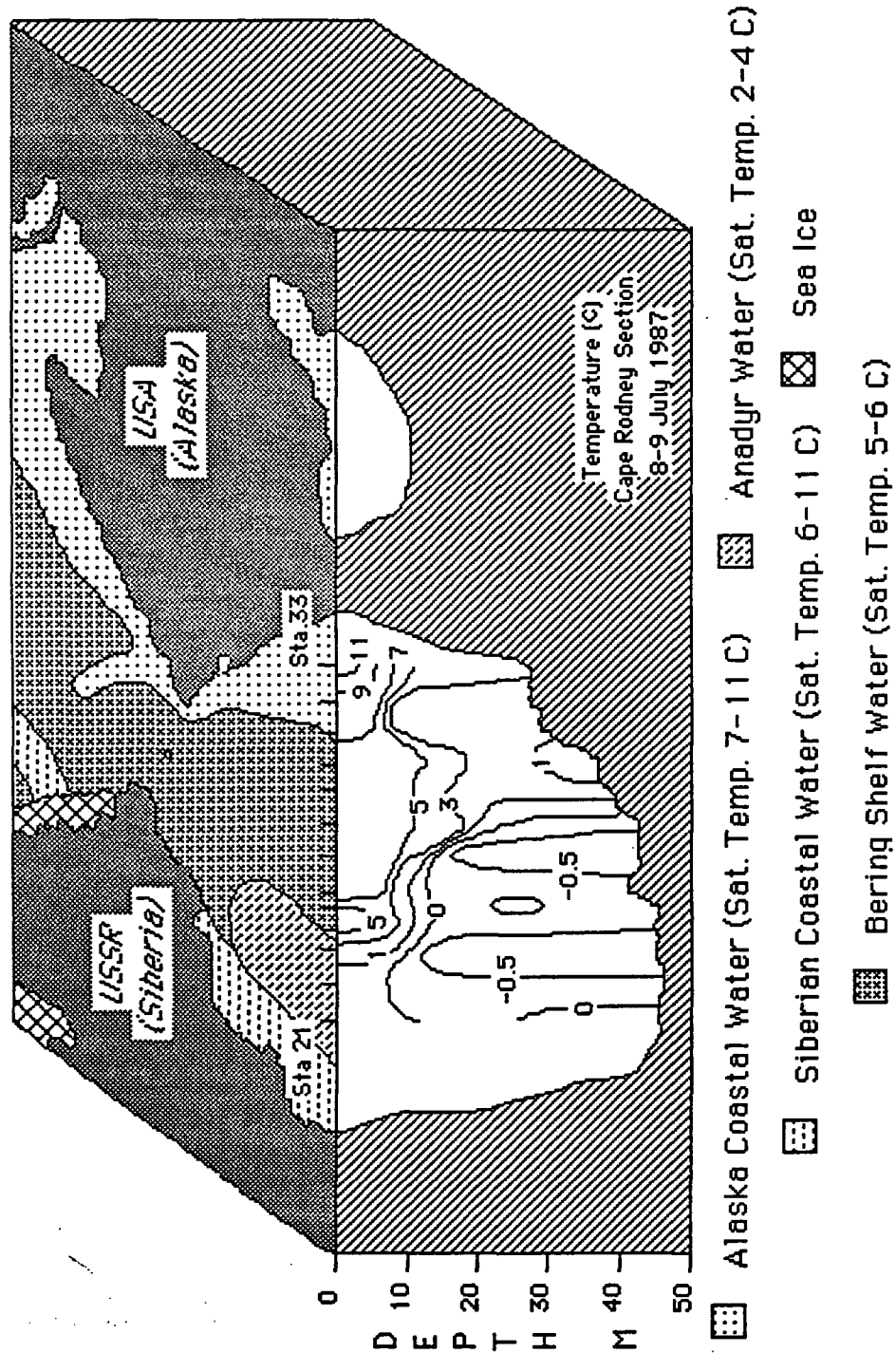
Figure 9. Block diagram showing the relationship between surface water bodies defined by sea surface temperatures observed on 8 July 87 AVHRR data and subsurface temperatures recorded on 8 & 9 July 87.
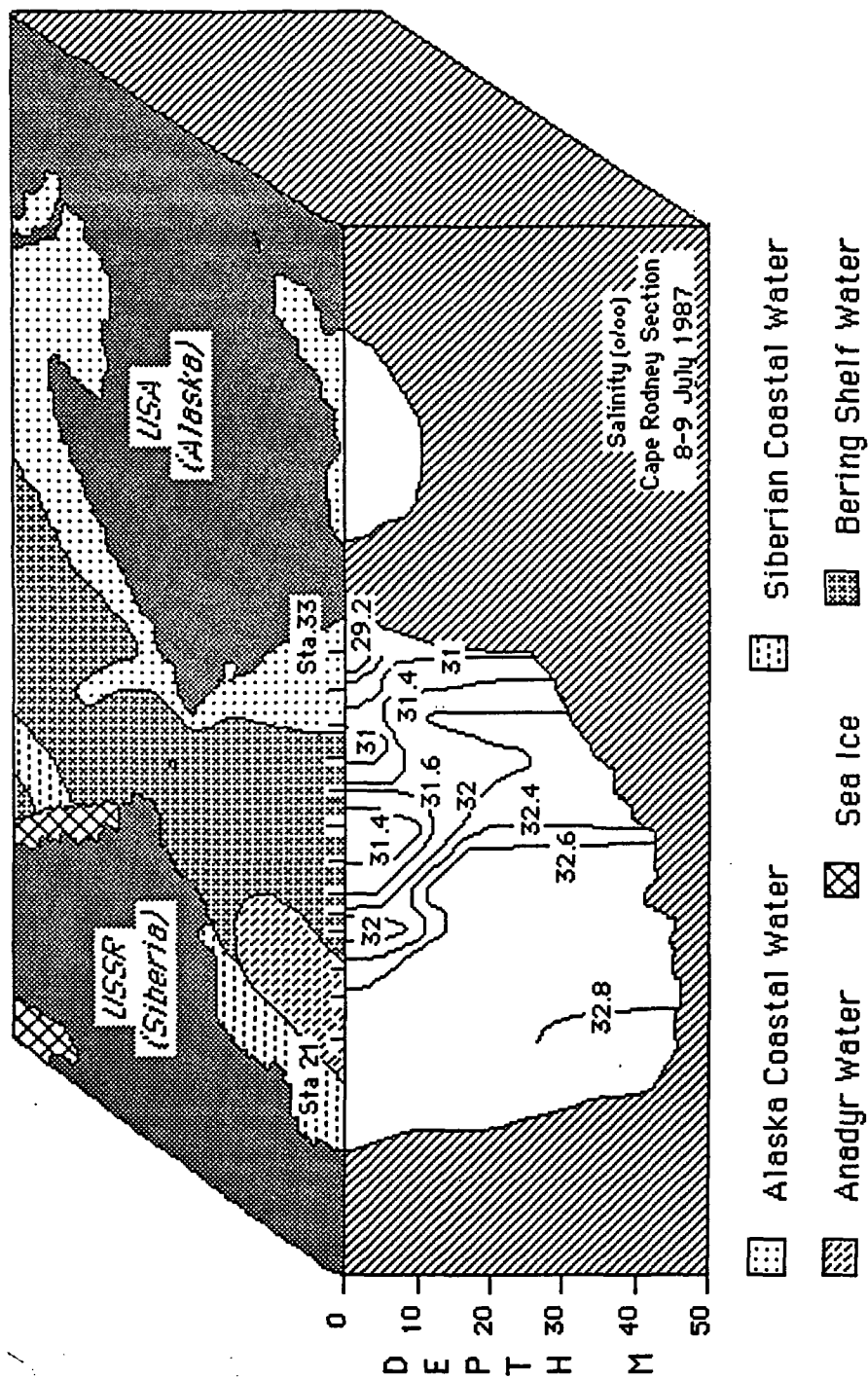
Figure 10. Block diagram showing the relationship between surface water bodies defined by sea surface temperatures observed on 8 July 87 AVHRR data and subsurface salinity measured on 8 & 9 July 1987.

15

3. The relatively high resolution of the TM thermal band reveals complex patterns and structures in the surface water that could not be resolved on previous data sets. The advection of warm coastal water into the Bering Sea results in intricate structures associated with mixing processes that can be observed on these images.

4. Analysis of historical images indicates only limited variation of the general pattern of warming over the years of 1974 to 1978. However, these variations could be crucial to ecological processes of the region and long term study in conjunction with oceanographic data collection is warranted.

5. Patterns of phytoplankton biomass and productivity in these shelf waters, as measured from ships, are determined by water mass distribution and hence are well correlated with the pattern if surface isotherm distribution obtained from satellite images.

ACKNOWLEDGMENTS

REFERENCES

Ahlnas, K. and Garrison, G.R. 1984. Satellite and oceanographic observations of the warm coastal current in the Chukchi Sea. Arctic, V. 37 (3), pp 244-254.

Burbank,D.C.,1974. Suspended sediment transport in Alaskan Coastal Waters. M.S. Thesis, University of Alaska Fairbanks, pp. 1-60.

Coachman, L.K., Aagaard, K. and Tripp, R.B. 1975, Bering Strait, the regional physical oceanography. University of Washington Press, Seattle, 172 pp.

Drake, D.E, D.A. Cacchione, R.D. Muench and C.H. Nelson, 1980. Sediment transport in Norton Sound, Alaska, Marine Geol. V. 36,   pp.97-128.

Dupre, W.R., 1982. Depositional environments of the Yukon Delta, northeastern Bering Sea, Geologie en Mi jnbouw, V.61(1), pp. 63-70.

Gosink, J. P., 1988. Buoyant surface jet analysis of the Yukon River, Int'l. Jour. of Remote Sensing, (in press).

NASA, 1984. A prospectus for thematic mapper research in the earth sciences, NASA Tech. Memo. 86149, pp. 18 & 19.

Nelson, C. H. 1982. Late Pleistocene transgressive sedimentation in deltaic and nondeltaic areas of the northeastern Bering epicontinental shelf, Geologie en Miubou, V.61 (1), pp.5-18.

Sharma, G. D., 1979. The Alaskan Shelf: hydrologic, sedimentary and geochemical environment, Springer-Verlag, New York, N.Y., USA, 498 pp.

Stringer B. S. and J. E. Groves, 1985. Statistical description of the summertime ice edge in the Chukchi Sea, Final report to U. S. Dept. of Energy, Contract # DE-AC21-83MC20037, 27 pp. + appendices.

Springer, A.M., E.C. Murphy, D.G. Roseneau, C.P. McRoy and B.A. Cooper, 1987. The paradox of pelagic food webs in the northern Bering Sea - I. Seabird food habits, Continental Shelf Research v.7(8), pp. 895-911.

Springer, A.M., D.G. Roseneau, E.C. Murphy and M.I. Springer, 1984. Environmental controls of marine food webs: Food habits of seabirds in the eastern Chukchi Sea, Can. J. Fish. Aquat. Sci. V. 41. pp. 1202-1215.

Thomas, I. L.,1980. Suspended sediment dynamics from repetitive Landsat data, Int'l. Jour. Remote Sensing, V. 1(13), pp. 285-292.

Tripp R.B., 1987. ISHTAR cruise report, Thomas G. Thompson cruise TT-212, 29 June to 19 July 1987, School of Oceanography, Univ. of Wash., Seattle, Wash. 98195, 47 pp.

U. S. Geol. Surv., 1975. Water resource data for Alaska, Water data report Ak-75-1, pp. 357-361.

U. S. Geol. Surv., 1976. Water resource data for Alaska, Water data report Ak-76-1, pp. 228-234.

U. S. Geol. Surv., 1977. Water resource data for Alaska, Water data report Ak-77-1, pp. 220-225.

U. S. Geol. Surv., 1978. Water resource data for Alaska, Water data report Ak-78-1, pp. 254-258.

ISHTAR. 1985. Data report. Institute of Marine Sciences, University of Alaska, Fairbanks.

APPENDIX

(Resulting Publications and Presentations)

Publications

Dean K.G. and McRoy, C.P., 1988. Distribution and circulation of turbid Yukon River water, (in preparation), 17pp.

Dean, K. G., McRoy, C.P., Ahlnas, K., and George T.H., 1987. Satellite observations of The northern Bering Sea. In: Proceedings of the Ninth Int'l Conf. on Port and Ocean Engineering under arctic conditions, Fairbanks, Alaska USA, August 17-22, 1987. Geophysical Institute, Univ. of Alaska, Fairbanks, Ak. (in press), 9 pp.

Gosink, J.P., 1987, Thermal plume analysis of the Yukon River, International Journal of Remote Sensing (in press).

McRoy, C.P., 1987. Global maximum of primary production in the Bering Sea (Abs), EOS, v68 (50), p.1727.

Walsh, J.J., McRoy,C.P., Coachman, L.K., GoeringJ.J., Nihoul, J.J., Whitledge, T.E., Blackburn, T.H., Parker, P.L.,Wirick, C.D., Shuert, P.G., Grebmeier, J.M., Springer, A.L., Tripp, R.D., Hansell, D., Djenidi, S., Deleersnijder, E., Henriksen, K., Lund, B.A., Andersen, P., Muller-Karger, F.E. and Dean K.G., 1988. Carbon and nitrogen cycling within the Bering/Chukchi Seas: source regions for matter affecting AOU demands of the Arctic Ocean. Submitted to Progress in Oceanography, approx. 80 pp. + maps and graphs.

Presentations

McRoy, C.P., 1988. Studies of the ecology of the shelf waters of the Bering and Chukchi Seas. Presented in Japan at:
      Tokyo University
      Japan National Polar Research Institute
      Institute of Low Temperature Sciences, Hokkaido Univ..

Dean, K. G., 1987. Satellite observations of The northern Bering Sea. Presented at: Proceedings of the Ninth Int'l Conf. on Port and Ocean Engineering under arctic conditions, Fairbanks, Alaska USA, August 17-22.

Dean, K.G., Satellite Observations of the Bering/Chukchi Seas. Presented at: Inner Shelf Transfer And Recycling (ISHTAR) Workshops on the Bering Sea:
      1985, New Orleans, La.
      1986, St. Petersburg, Fl.
      1987, Corpus Christi, Tx.

Dean, K.G., Influence of the Yukon River on the Bering Sea. Presented at: Landsat TM Investigators Workshops:
      1985, Indianapolis, In.
      1986, NASA-GSFC, Greenbelt, Md.
      1987, UCSB, Santa Barbara, Ca.